

Article

Optimization of High-Temperature CO₂ Capture by Lithium Orthosilicate-Based Sorbents Using Response Surface Methodology

Eleonora Stefanelli, Flavio Francalanci, Sandra Vitolo  and Monica Puccini * 

Department of Civil and Industrial Engineering, University of Pisa, Largo Lucio Lazzarino 1, 56122 Pisa, Italy; eleonora.stefanelli@unipi.it (E.S.); f.francalanci1@studenti.unipi.it (F.F.); sandra.vitolo@unipi.it (S.V.)

* Correspondence: monica.puccini@unipi.it; Tel.: +39-0502217888

Abstract: The major challenge in the current context of the rising world energy demand is to limit the global temperature increase for mitigating climate change. This goal requires a large reduction of CO₂ emissions, mainly produced by power generation and industrial processes using fossil fuels. In this study, a novel methodology for K₂CO₃-doped Li₄SiO₄ sorbents production for CO₂ capture at high temperatures was adopted based on the Design of Experiments (DoE). This innovative approach systematically tested different synthesis (temperature and K₂CO₃ content) and adsorption conditions (sorption temperature and CO₂ concentration), allowing for the assessment of individual and interactive effects of process parameters. The Response Surface Methodology (RSM) was employed to obtain non-linear predictive models of CO₂ uptake and Li₄SiO₄ conversion. The results of RSM analysis evidenced a maximum adsorption capacity of 196.4 mg/g for a sorbent produced at 600 °C and with 36.9 wt% of K₂CO₃, tested at 500 °C and 4 vol% of CO₂. Whereas at 50 vol% of CO₂, the best uptake of 295.6 mg/g was obtained with a sorbent synthesized at 600 °C, containing less K₂CO₃ (17.1 wt%) and tested at a higher temperature (662 °C). These findings demonstrate that K₂CO₃-doped Li₄SiO₄ sorbents can be tailored to maximize CO₂ capture under various operating conditions, making them suitable for use in industrial processes.

Keywords: solid sorbent; lithium orthosilicate; CO₂ capture; high temperature; adsorption; Design of Experiments



Citation: Stefanelli, E.; Francalanci, F.; Vitolo, S.; Puccini, M. Optimization of High-Temperature CO₂ Capture by Lithium Orthosilicate-Based Sorbents Using Response Surface Methodology. *Atmosphere* **2024**, *15*, 908. <https://doi.org/10.3390/atmos15080908>

Academic Editor: Dezhong Yang

Received: 28 June 2024

Revised: 17 July 2024

Accepted: 21 July 2024

Published: 30 July 2024



Copyright: © 2024 by the authors. Licensee MDPI, Basel, Switzerland. This article is an open access article distributed under the terms and conditions of the Creative Commons Attribution (CC BY) license (<https://creativecommons.org/licenses/by/4.0/>).

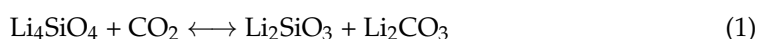
1. Introduction

Carbon dioxide (CO₂) emissions due to anthropogenic activities play a significant role in global warming and climate change. Nowadays, the CO₂ concentration in the atmosphere is rising at a rate of 2 ppm per year [1,2]. This progressive increase is responsible for climate change, which has a critical effect on global environmental processes such as the long-term increase of the global temperature [3], melting of polar ice [2], severe weather events, and much more [4,5]. To mitigate the effect of human activities, renewable energy sources are becoming more widespread; however, fossil fuels and natural gas remain the primary sources of energy [6–8]. Therefore, developing novel and economically viable technologies for reducing CO₂ emissions is essential [9].

Carbon Capture and Storage (CCS), particularly post-combustion CO₂ capture, is one of the most promising techniques to reduce emissions in the hard-to-abate sectors [10,11]. CCS offers a feasible pathway for separating CO₂ from exhaust gases without requiring substantial changes to the existing chemical processes. High-temperature selective adsorption by employing solid sorbents is gaining attention as an effective approach for capturing CO₂ from gas streams in industrial processes [12]. In recent years, numerous studies have focused on the use of solid sorbents for CO₂ adsorption, such as CaO-based [13–15], Li-based [16–21], or Na-based sorbents [22,23]. Among these, lithium orthosilicate (Li₄SiO₄) emerges as a key material for such applications due to its high theoretical adsorption capacity (367 mg CO₂/g sorbent) than other alkaline ceramics, such as lithium zirconate

(Li_2ZrO_3) and sodium zirconate (Na_2ZrO_3), which can adsorb 287 and 237 mg/g, respectively. Additionally, the cost of raw materials for Li_2ZrO_3 and Na_2ZrO_3 synthesis is higher due to the expensive nature of ZrO_2 , in contrast to the more economical SiO_2 used in Li_4SiO_4 . Moreover, Li_2ZrO_3 demonstrates a slower sorption rate under comparable conditions, while Na_2ZrO_3 exhibits poorer regeneration performance due to sintering effects, in comparison to Li_4SiO_4 [23]. Furthermore, Li_4SiO_4 presents a wide adsorption temperature range (450–700 °C) and excellent regenerability at lower temperatures than those required by other absorbents (e.g., CaO) [17,24,25]. Calcium oxide offers advantages such as low raw material costs, as well as high CO_2 adsorption capacity and sorption rate. However, its industrial application faces significant challenges, including the requirement for a high regeneration temperature (>800 °C) and a substantial reduction in adsorption capacity over long-term operation due to sintering phenomena [23].

The CO_2 adsorption-desorption process by Li_4SiO_4 can be described by the reversible reaction:



that leads to the formation of two solid products, lithium metasilicate (Li_2SiO_3) and lithium carbonate (Li_2CO_3). The adsorption process can be divided into two stages: a first initial fast chemical regime, where CO_2 reacts directly with Li_4SiO_4 , forming a products layer on the surface of the sorbent particles, followed by a diffusive stage, where CO_2 must diffuse through the products layer to continue the reaction [26]. At low CO_2 partial pressures, typical of industrial flue gas emissions, Li_4SiO_4 adsorption kinetics is limited due to the slow diffusion of CO_2 throughout the solid layer. Therefore, to overcome this issue, several strategies for enhancing its reactivity have been proposed, such as the addition of alkali carbonates (potassium carbonate, K_2CO_3 , or sodium carbonate, Na_2CO_3). These additives form eutectic carbonate mixtures with the Li_2CO_3 product resulting from the carbonation reaction that melts at the sorption temperatures [27–30]. The molten eutectic mixtures facilitate CO_2 diffusion through the product layer, significantly enhancing the adsorption rate. Thus, alkali-doped Li_4SiO_4 results promising for CO_2 capture, especially at the low CO_2 concentrations typical of exhaust hot gases from gas turbines.

As evidenced by recent reviews [17,24,25], CO_2 adsorption by Li_4SiO_4 is greatly affected by the operating conditions of the process (adsorption temperature and CO_2 concentration). Moreover, the adsorption performance is also influenced by the microstructure of the sorbent (such as particle size, surface area, and porosity), which mainly depends on the sorbent synthesis condition and the doping method used. Nevertheless, up to the present time, doped- Li_4SiO_4 adsorption capacities were investigated through a One factor at a Time (OFAT) methodology, thus making only one process parameter varying at a time focusing on its individual effect on CO_2 removal [19,27–29,31–34]. Since these variables could have interactions with each other, the optimization of the process is not easy.

The Design of Experiments (DoE) is based on a statistical approach carried out by randomized experiment planning that allows to evaluate both individual and interactive effects of process parameters, which is very different from the typical deterministic approach of OFAT methods. The latter generally requires a large number of tests to evaluate the effect that a given input can have on the output of a process, leading to conclusions with a limited validity range. Instead, a factorial design (a typical example of DoE) allows to develop a more robust model of the process by minimizing the number of tests required and, therefore, optimizing the resources available [35–38]. A good experimental design must avoid systematic error, allow estimation of the experimental error (pure, random error), and have broad validity [39].

In this work, Li_4SiO_4 -based sorbents were fabricated using a solid-state methodology that started from lithium hydroxide, LiOH , and silica, SiO_2 . Solid-state doping with K_2CO_3 was employed for obtaining a sorbent with high CO_2 capture capacity. Systematic fabrication tests were conducted applying the DoE methodology to identify the sorbents synthesis conditions (such as the synthesis temperature and K_2CO_3 content) and the adsorption process operating conditions (like CO_2 concentration and adsorption temperature)

that mostly affect the adsorption performance of the K_2CO_3 -doped Li_4SiO_4 sorbents. A Response Surface Method (RSM) design was then executed to evaluate the interactions among the synthesis and process variables and to identify the factors that significantly influence the doped sorbent performance, i.e., the Li_4SiO_4 conversion and the adsorption capacity. The RSM analysis provided parametric models that were used to find optimal conditions for maximizing the adsorption performance of Li_4SiO_4 -based sorbents at different concentrations of CO_2 .

2. Materials and Methods

2.1. Sorbents Production and Characterization

The production of Li_4SiO_4 -based sorbents was carried out using a solid-state method already tuned in a previous work of the research group [27], starting from lithium hydroxide (LiOH, powder, reagent-grade, Sigma-Aldrich, St. Louis, MO, USA) and crystalline silicon dioxide (SiO_2 , 0.5–5 μm powder, Sigma-Aldrich) as reagents. For each experiment, 3 g of total reagent powders were mixed with 5 mL of distilled water in a ceramic mortar using a Li:Si molar ratio of 2:1. The obtained slurry was ground with a pestle for about 10 min, then dried at 90 °C overnight, and calcined in air in a muffle furnace. The calcining temperature was selected as a variable in the DoE study and ranged from 600 to 900 °C, while calcining time was set to 10 h. After that, the calcined powders were mixed with potassium carbonate (K_2CO_3 , powder, reagent-grade, Sigma-Aldrich) as activity promoter, finally obtaining the doped sorbents. The amount of K_2CO_3 was varied between 10 and 40 wt% (by weight of Li_4SiO_4), as it was also selected as a design variable.

The produced sorbents were characterized by X-ray diffraction (XRD) to evaluate the phase composition and assess Li_4SiO_4 formation for each fabrication condition. The diffractometer used was a Bruker D2 Phaser (Bruker Corporation, Billerica, MA, USA) using a Cu-K α radiation and a Ni filter equipped with a Lynxeye detector. The analysis was conducted over a 2θ range between 15° and 65° at a pitch of 0.02°. The sorbents' morphology was also investigated employing scanning electron microscopy (SEM) using a FEI Quanta FEG 450 (FEI Inc., Hillsboro, OR, USA). Prior to the analysis, each sample was coated with a thin gold layer to avoid charge build up.

2.2. CO_2 Capture Experiments Setup and Procedure

The carbon dioxide adsorption performance of Li_4SiO_4 -based sorbents was determined by isothermal tests conducted in a thermogravimetric analyzer (TGA, Q500 TA Instruments, New Castle, DE, USA) varying the adsorption temperature and CO_2 concentration in the treated gas according to the DoE matrix. For each experiment, approximately 20 mg of powder was placed in a platinum sample pan and first pre-conditioned in nitrogen flow (100 mL/min) raising the temperature with a heating rate of 20 °C/min to the selected adsorption temperature (varied between 500 and 700 °C). Then, the gas stream was changed into a CO_2/N_2 mixture with different concentrations (4–50 vol% of CO_2) and a total flow rate of 100 mL/min at atmospheric pressure. The increase in sample weight resulting from CO_2 adsorption was monitored over time, and the CO_2 uptake was calculated as in Equation (2):

$$CO_2 \text{ uptake (mg/g)} = \frac{(m_t - m_0)}{m_0} \cdot 1000 \quad (2)$$

where m_t is the sample mass at generic time t (mg), and m_0 is the initial sample mass (mg). The sorbent's adsorption capacity was then evaluated as the CO_2 uptake after 120 min of adsorption. Moreover, the Li_4SiO_4 conversion was determined by TGA tests according to Equation (3):

$$X_{Li_4SiO_4}(\%) = \frac{CO_2 \text{ uptake}}{f_{Li_4SiO_4} \cdot C_{ST}} \cdot 100 \quad (3)$$

where $f_{Li_4SiO_4}$ is the mass fraction of Li_4SiO_4 in the sorbent and C_{ST} is the theoretical CO_2 uptake of Li_4SiO_4 (367 mg/g Li_4SiO_4). After the adsorption process, lasting 120 min,

the sorbent was regenerated by converting the feed gas to 100% N₂ and maintaining the temperature at 700 °C for 30 min.

2.3. Experimental Design and Parametric Models

The Design of Experiments is an analytical method that allows to evaluate the effect due to input parameters of a process (variables, or factors) on the outputs (responses) through the development of a probabilistic model able to predict the desired responses. For this study, DoE methodology has been applied to evaluate the sorbent performances and to select optimal production parameters to maximize CO₂ removal. The randomized runs for the experimentation and the model construction were attained using Design Expert (Version 11) software. Four factors were selected as significant for the adsorption process among all the variables involved in the synthesis of the sorbent and in the adsorption phase (Table 1): synthesis temperature (600–900 °C), K₂CO₃ content (10–40 wt%), adsorption temperature (500–700 °C), and CO₂ concentration (4–50 vol%). The synthesis time was not considered for the DoE analysis since it was found to be negligible, according to preliminary evaluations. A RSM approach was applied in order to find non-linear interactions between the factors, following a 2⁴ full-factorial face-centered Central Composite Design (CCD). The experimental matrix was determined using Equation (4):

$$N = 2^n + 2n + n_c \quad (4)$$

where N is the total experimental runs required for a full-factorial CCD, n is the variables number, $2n$ is the number of axial runs, and n_c is the number of replicates on the central point (i.e., conducted at the center of the design). The design matrix (Table 2) was thus constituted of 30 total runs, including 16 runs at factorial points, 8 runs at axial points, and 6 replicates at the central point.

Table 1. Variable levels used in the RSM experimental design.

Variables (Factors)	Unit	Levels		
		−1	0	+1
Synthesis temperature	°C	600	750	900
K ₂ CO ₃ content	wt%	10	25	40
Adsorption temperature	°C	500	600	700
CO ₂ concentration	vol%	4	27	50

Table 2. Experimental design matrix and responses results for RSM design of experiments.

Run	Input Variables				Responses	
	A Synthesis Temperature (°C)	B K ₂ CO ₃ Content (wt%)	C Adsorption Temperature (°C)	D CO ₂ Concentration * (vol%)	Y ₁ X _{Li4SiO4} (%)	Y ₂ Adsorption Capacity (mg/g)
1	750	25	600	27	76.32	224.15
2	750	25	700	27	75.78	222.58
3	750	25	600	50	66.54	195.44
4	600	10	500	50	66.76	222.80
5	750	25	600	27	69.37	203.73
6	900	10	500	50	35.61	118.86
7	750	25	600	27	66.50	195.30
8	600	40	700	50	96.88	254.07
9	750	25	600	27	64.30	188.86
10	900	40	500	4	41.36	108.45
11	750	25	600	4	49.16	144.38
12	600	40	500	50	78.50	205.85
13	900	40	500	50	39.76	104.27
14	900	10	500	4	31.37	104.71
15	750	40	600	27	62.56	164.05

Table 2. Cont.

Run	Input Variables				Responses	
	A Synthesis Temperature (°C)	B K ₂ CO ₃ Content (wt%)	C Adsorption Temperature (°C)	D CO ₂ Concentration * (vol%)	Y ₁ X _{Li₄SiO₄} (%)	Y ₂ Adsorption Capacity (mg/g)
16	750	25	500	27	43.77	128.56
17	900	10	700	50	93.54	312.19
18	600	25	600	27	92.26	270.98
19	600	40	500	4	72.95	191.36
20	600	10	700	4	3.390	11.310
21	750	25	600	27	65.93	193.62
22	900	40	700	50	95.89	251.45
23	750	25	600	27	64.67	189.95
24	900	40	700	4	26.19	68.670
25	750	10	600	27	58.39	194.87
26	900	10	700	4	6.600	22.030
27	600	10	700	50	92.20	307.72
28	600	10	500	4	58.90	196.58
29	600	40	700	4	23.40	61.330
30	900	25	600	27	65.60	192.67

* The values of CO₂ concentration levels used for the experimental design were adjusted to the real CO₂ concentration in the inlet gas flow in the thermogravimetric analyzer measured with flowmeters: (−1) level corresponded to 4.1 vol%, (0) level corresponded to 25.8 vol% and (+1) level corresponded to 47.5 vol%. The real values were used in the design to minimize the pure error and obtain a more predictive model of the responses.

The responses chosen to evaluate the sorbent performances were Li₄SiO₄ conversion (Y₁) and sorbent's adsorption capacity (Y₂), expressed as in Equations (3) and (2), respectively. Both values of responses were taken at the end of the adsorption isotherm (120 min), when the reaction was supposed to have reached equilibrium. The responses results from the RSM experimental design are reported in Table 2. For each response, the analysis of variance (ANOVA) was performed to find parametric models that best fit the experimental data. The second-order general equation obtained for the responses is shown in Equation (5):

$$Y = \beta_0 + \sum_{i=1}^k \beta_i x_i + \sum_{i=1}^k \beta_{ii} x_i^2 + \sum_{1 < i < j}^k \beta_{ij} x_i x_j \quad (5)$$

where β_0 is the constant coefficient that corresponds to the overall mean of the experimental data, β_i are the linear coefficients of x_i , which is the i -th variable of the experimental design, β_{ii} are the quadratic coefficients, and β_{ij} are the two-factor interaction coefficients.

3. Results and Discussion

3.1. Sorbents Characterization

The pure Li₄SiO₄ powders obtained in each run of the experimental design (both for the preliminary screening and the RSM design) were analyzed by XRD to verify the formation of the lithium orthosilicate phase. Figure 1 reported, as an example, the diffractograms of the sorbents obtained by the RSM experimentations calcined for 10 h at different temperatures (600–900 °C). As shown, the sorbents exhibited a pattern with major peaks of the Li₄SiO₄ crystalline phase, confirming that the selected temperatures were sufficient for assessing the sorbent synthesis. The sorbent calcined at 600 °C presented small peaks attributable to the reagent lithium carbonate. The presence of Li₂CO₃ is probably attributed to an incomplete conversion of SiO₂ and LiOH due to the low synthesis temperature; LiOH is then carbonated owed to contact with air during calcining [27,40].

The Li₄SiO₄ powders were also characterized by SEM to assess the sorbents morphology and particle dimensions. Figure 2 displays SEM images of the pure sorbents calcined for 10 h at different temperatures (relative to samples 10, 11, and 19 of the experimental runs of Table 2). The sorbent calcined at 600 °C (Figure 2a,d) showed dense and non-porous particles with sizes below 5 µm agglomerated in clusters of very large dimensions (greater

than 100 μm). By increasing the calcining temperature to 750 and 900 $^{\circ}\text{C}$, the Li_4SiO_4 sorbents presented a significant sintering of the particles, showing essentially a non-porous particle morphology and greater diameters of about 30–50 μm .

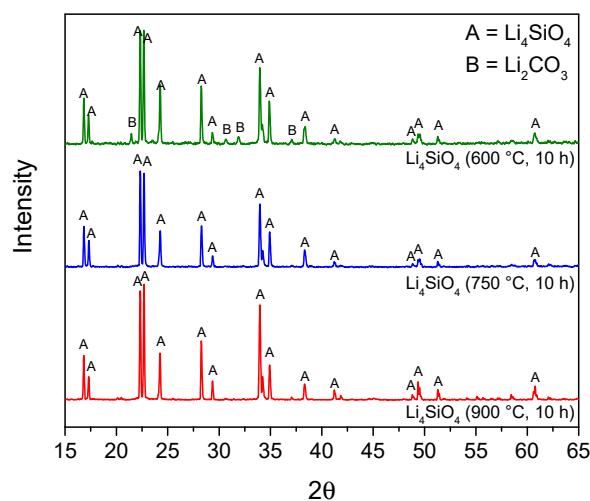


Figure 1. X-ray diffraction patterns for the synthesized sorbents at different temperatures: Li_4SiO_4 (600 $^{\circ}\text{C}$, 10 h) is the sample of run 19, Li_4SiO_4 (750 $^{\circ}\text{C}$, 10 h) is run 11, and Li_4SiO_4 (900 $^{\circ}\text{C}$, 10 h) is run 10 of the experimental design matrix.

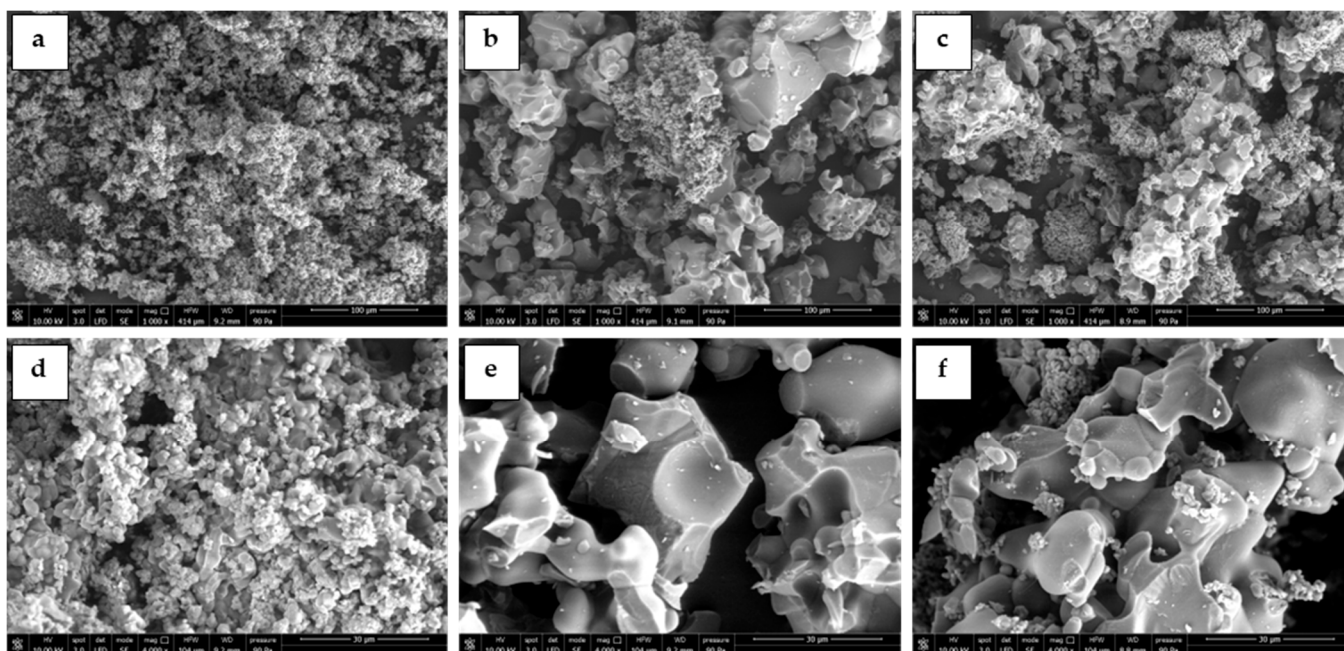


Figure 2. SEM images of the pure Li_4SiO_4 sorbents synthesized for 10 h at different temperatures: (a,d) 600 $^{\circ}\text{C}$, (b,e) 750 $^{\circ}\text{C}$, and (c,f) 900 $^{\circ}\text{C}$. Images obtained at different magnifications: first row 1000 \times and second row 4000 \times .

Moreover, Figure 3 reports images of the morphology of the doped sorbents calcined at different temperatures obtained by SEM analysis. For example, the sorbent with 10 vol% of potassium carbonate was analyzed. All the doped sorbents showed the same morphology and particle size evidenced for the pure Li_4SiO_4 , demonstrating that the solid-state doping method did not affect the overall structure of the sorbent. K_2CO_3 was constituted by porous particles that were well distributed among the dense Li_4SiO_4 particles, as can be seen in Figure 3b,c.

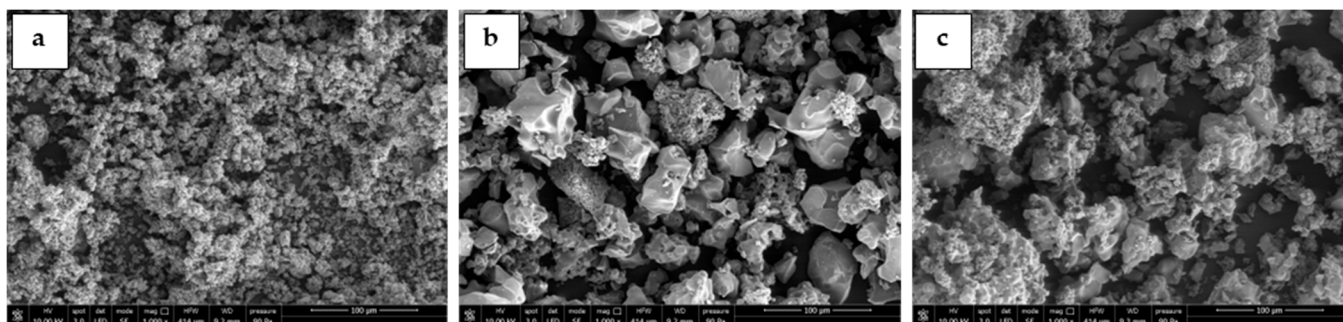


Figure 3. SEM images of the doped Li_4SiO_4 sorbents (10 wt% of K_2CO_3) synthesized at different temperatures for 10 h: (a) 600 °C, (b) 750 °C, and (c) 900 °C.

3.2. Preliminary Variables Selection for Parametric Modeling

To fully comprehend the adsorption process of doped Li_4SiO_4 sorbents and how it is influenced by the sorbent's synthesis and process conditions, a DoE methodology was applied. Initially, five variables were selected as potentially significant for the adsorption process. The variables concerned both the sorbent preparation conditions and the adsorption operating conditions: calcining temperature and time, K_2CO_3 content, adsorption temperature, and CO_2 concentration. For the synthesis temperature, the low level was set to 600 °C since it represents the minimum temperature necessary for the Li_4SiO_4 synthesis from the precursors [41], while the high level (900 °C) is the typical synthesis temperature for a solid-state method. A higher value could lead to Li_4SiO_4 decomposition to Li_2SiO_3 by lithium sublimation [42]. The calcining time was varied from 4 h, which is a typical synthesis time used in literature for a complete conversion of reagents to Li_4SiO_4 [43], to 10 h. A longer synthesis time was not considered since, at 900 °C, could promote lithium sublimation [42]. The K_2CO_3 content was chosen from a previous study on Li_4SiO_4 -based sorbents [44]. A promoter amount exceeding 40 wt% was not considered appropriate since it would reduce the amount of active sorbent.

The CO_2 concentration in vol% refers to the volume fraction of CO_2 in the TGA feed gas, consisting of a CO_2/N_2 mixture flow. The low level was set to 4 vol% (corresponding to a CO_2 partial pressure of 0.04 atm), which is typical of exhaust hot gases from gas turbines [45–48], while the high level (50 vol%) depended on the thermogravimetric analyzer operating limit. Then, the adsorption temperature range (500–700 °C) was chosen considering the curve of the equilibrium partial pressure of CO_2 at different temperatures, which has been evaluated on the basis of the Gibbs free energy changes of the adsorption/desorption reaction (Equation (1)) [49]. The heterogeneous reaction that occurs between Li_4SiO_4 and CO_2 is an equilibrium reaction; therefore, for each CO_2 partial pressure, there is a thermodynamic equilibrium temperature below which the sorption reaction could proceed ($\Delta G < 0$); otherwise, the desorption process takes place ($\Delta G > 0$). At the equilibrium of Equation (1), the following equation can be valid since $\Delta G = 0$ is satisfied:

$$\Delta G_r^0(T) = \Delta H_r^0(T) - T \cdot \Delta S_r^0(T) = -RT \ln(K_{eq}) \quad (6)$$

where ΔG_r^0 , ΔH_r^0 , and ΔS_r^0 represent the variation of standard Gibbs energy, standard enthalpy, and standard entropy of the carbonation reaction, respectively; R is the ideal gas constant; and T is the temperature. K_{eq} is the equilibrium constant for the reaction (Equation (1)) and is defined as in Equation (7):

$$K_{eq} = \frac{1}{p_{\text{CO}_2}} \quad (7)$$

where p_{CO_2} is the CO_2 partial pressure in the treated gas.

The p_{CO_2} –temperature equilibrium curve can be evaluated from Equations (6) and (7), as found in a previous work of the authors [49], and it is reported in Figure 4. As shown,

the two-dimensional design space (for the two factors of adsorption temperature and CO₂ concentration) covers the entire region where the adsorption reaction is activated both at the low and high CO₂ concentration levels (4 and 50 vol%).

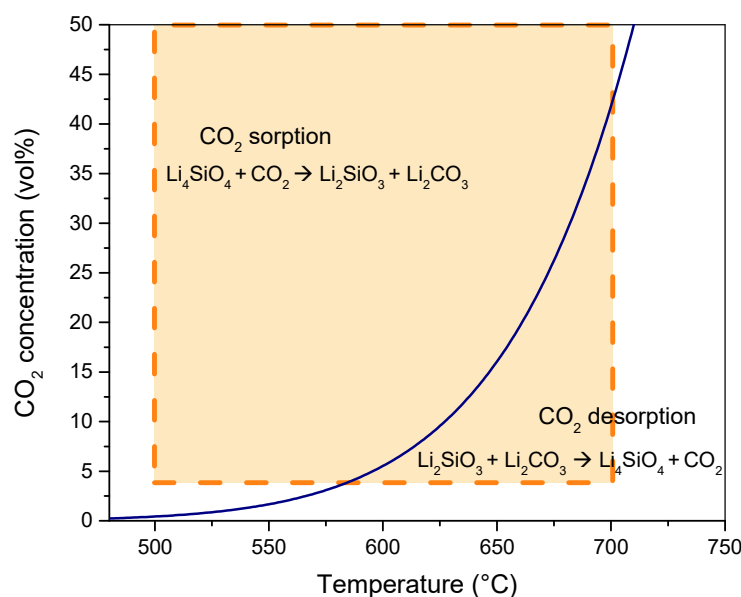


Figure 4. Equilibrium CO₂ concentration at different temperatures for CO₂ adsorption reaction with Li₄SiO₄. (The orange rectangle represents the design space for the two factors of adsorption temperature and CO₂ concentration).

Preliminary calcining and adsorption tests were conducted with experimental tests using TGA to assess the effect of calcining time on the synthesis and the adsorption performance of the sorbent. Calcining in TGA was performed by placing the mixed reagent powders in the platinum crucible and heating them to the selected synthesis temperature (600 or 900 °C) under air flow. The temperature was maintained for several hours to observe the weight loss during the synthesis reaction. The results are reported in Figure 5. As shown, the main difference among the two thermograms (Figure 5a,b) was related to the synthesis temperature. A weight loss was observed in the range between 400 and 600 °C and this was attributed to the LiOH decomposition to lithium oxide, Li₂O [40]. Therefore, when the Li₄SiO₄ synthesis took place at 600 °C, the time needed to reach the complete LiOH decomposition and, supposedly, the complete conversion of reagents was higher than for the synthesis at 900 °C, where the sample weight became stable even before reaching the isotherm section. Whereas, for the same synthesis temperature, the synthesis time (4 or 10 h of isotherm) did not affect markedly the conversion of reagents. A variation in weight loss less than 0.5% was observed from 4 to 10 h.

Moreover, preliminary adsorption tests were carried out on 10 wt% K₂CO₃ doped-Li₄SiO₄ sorbents prepared with different synthesis times and temperatures. The results of the adsorption experiments in terms of both adsorption capacity and Li₄SiO₄ conversion are reported in Figure 6, considering an adsorption temperature of 500 °C and a CO₂ concentration of 4 vol%.

As illustrated, the adsorption performance was almost unchanged by varying the calcining time from 4 to 10 h. The main difference in the CO₂ uptake could be ascribed to the calcining temperature effect. An increase in the calcining temperature from 600 to 900 °C led to a decrease in the adsorption capacity and sorbent conversion, which changed from about 240 to 200 mg/g and from 73 to 62%, respectively. These preliminary results are in accordance with the adsorption capacities of K₂CO₃-doped Li₄SiO₄ sorbents reported in recent literature. Zhang et al. [30] and Wang et al. [29] prepared sorbents by the solid-state method doped with K₂CO₃ (17.5 and 10 wt%, respectively), obtaining a CO₂ uptake of

276.7 and 239.6 mg/g, respectively. Nevertheless, it is important to highlight that these adsorption capacities have been obtained at 600 °C and 20 vol% of CO₂ in the treated gas. According to Figure 6 results, the produced sorbents present a better adsorption capacity since they can achieve the same uptake even at much lower CO₂ content.

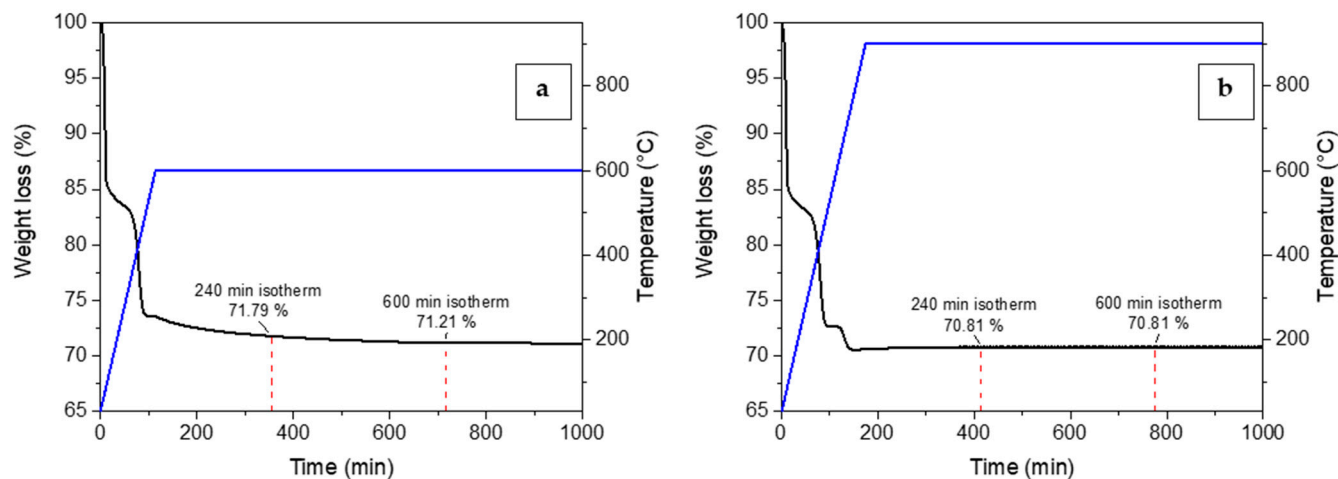


Figure 5. Weight loss (black line) and temperature profiles (blue line) vs time for the calcination of Li₄SiO₄ in the thermogravimetric analyzer at (a) 600 and (b) 900 °C.

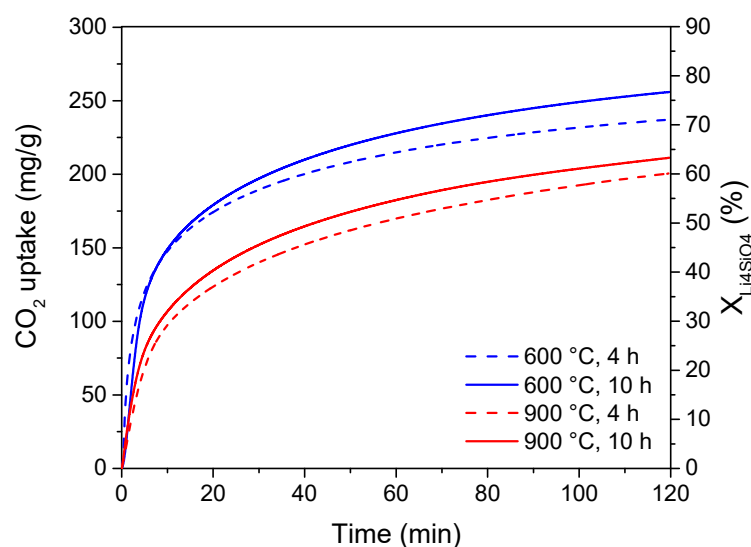


Figure 6. CO₂ adsorption profiles at 500 °C and 4 vol% CO₂ stream of 10 wt% K₂CO₃ doped-Li₄SiO₄ synthesized at different temperatures (600, 900 °C) and times (4, 10 h).

Further considerations on the calcining temperature effect will be dealt with in the modeling section. These experimental considerations evidence that the synthesis time was poorly significant in affecting the adsorption performance of the sorbent. Therefore, it was not considered in the following RSM analysis and was set to a value that allowed us to obtain a complete conversion of the reactants into Li₄SiO₄ for all the synthesis temperatures of the design space. Thus, a synthesis time of 10 h was selected, and the five variables were consequently reduced to four.

3.3. Modeling of the CO₂ Adsorption Process and Statistical Analysis

A Response Surface Method DoE was conducted to investigate the combined effect of the variables on the adsorption process and to develop non-linear models of the selected responses Li₄SiO₄ conversion and sorbent's adsorption capacity. The obtained experimental

design matrix along with the responses results are reported in Table 2. Using the software Design Expert 11, regression calculations were executed to find the polynomial model that best fits the experimental data for each response. The analysis of variance (ANOVA) was conducted to confirm the statistical significance of all terms in the regression models, by means of statistical parameters. Each term of the resulting models corresponds to a main or interaction effect of a variable (or combination of variables) on the response. ANOVA splits data variability into two sources of variation, the model and the experimental error, and it uses F-values and *p*-values calculated for each term to verify their significance. Significant model terms were considered the ones having a *p*-value < 0.05. The goodness of models also depends on the determination coefficient R^2 and on its modification, adjusted R^2 , which only increases when terms really affecting the model are selected. Predicted R^2 was also checked as a measure of the predictivity of the model. ANOVA results and modeling statistics related to the RSM design for both responses are shown in Tables 3 and 4.

Table 3. ANOVA results and modeling statistics of Li_4SiO_4 conversion (Y_1) for RSM DoE.

	Sum of Squares	df	Mean Square	F-Value	<i>p</i> -Value	
Model	18,056.83	14	1289.77	80.42	<0.0001	significant
A-Synthesis temperature	1238.99	1	1238.99	77.25	<0.0001	
B- K_2CO_3 content	457.49	1	457.49	28.52	<0.0001	
C-Adsorption temperature	512.43	1	512.43	31.95	<0.0001	
D- CO_2 concentration	151.10	1	151.10	9.42	0.0078	
AC	1145.37	1	1145.37	71.41	<0.0001	
AD	16.81	1	16.81	1.05	0.3221	
BD	103.61	1	103.61	6.46	0.0226	
CD	5735.35	1	5735.35	357.60	<0.0001	
A^2	325.90	1	325.90	20.32	0.0004	
B^2	135.92	1	135.92	8.48	0.0107	
C^2	163.32	1	163.32	10.18	0.0061	
D^2	252.20	1	252.20	15.73	0.0012	
A^2C	410.97	1	410.97	25.62	0.0001	
A^2D	266.52	1	266.52	16.62	0.0010	
Residual	240.57	15	16.04			not significant
Lack of fit	138.33	10	13.83	0.6765	0.7204	
Pure error	102.24	5	20.45			
Cor Total	18,297.40	29				
Model statistics						
R^2	0.9869					
Adjusted R^2	0.9746					
Predicted R^2	0.9602					

Table 4. ANOVA results and modeling statistics of adsorption capacity (Y_2) for RSM DoE.

	Sum of Squares	df	Mean Square	F-Value	<i>p</i> -Value	
Model	$1.599 \cdot 10^5$	13	12,300.57	41.24	<0.0001	significant
A-Synthesis temperature	10,692.54	1	10,692.54	35.85	<0.0001	
B- K_2CO_3 content	369.47	1	369.47	1.24	0.2821	
C-Adsorption temperature	4420.24	1	4420.24	14.82	0.0014	
D- CO_2 concentration	1303.36	1	1303.36	4.37	0.0529	
AC	10,010.29	1	10,010.29	33.56	<0.0001	
AD	137.69	1	137.69	0.4617	0.5066	
BD	3633.50	1	3633.50	12.18	0.0030	
CD	51,918.23	1	51,918.23	174.08	<0.0001	
A^2	2018.70	1	2018.70	6.77	0.0193	

Table 4. Cont.

	Sum of Squares	df	Mean Square	F-Value	p-Value	
C ²	2485.75	1	2485.75	8.33	0.0107	
D ²	3527.27	1	3527.27	11.83	0.0034	
A ² C	3563.28	1	3563.28	11.95	0.0032	
A ² D	2536.04	1	2536.04	8.50	0.0101	
Residual	4771.81	16	298.24			
Lack of fit	3889.86	11	353.62	2.00	0.2288	not significant
Pure error	881.95	5	176.39			
Cor Total	1.647·10 ⁵	29				
Model statistics						
R ²	0.9710					
Adjusted R ²	0.9475					
Predicted R ²	0.8237					

For both Li₄SiO₄ conversion and adsorption capacity, a quadratic model with additional mid-cubic terms was found to best fit the experimental data. The ANOVA results showed that the models were both statistically significant (p -value < 0.05). Moreover, no significant lack of fit denoted the reliability of their predictive quality (p -value > 0.1). An estimation of pure error was also reported and evaluated through the replicates on the central points. The sum of squares of pure error was found to be at least two orders of magnitude lower than that of the models, representing their goodness in fitting the experimental data. High values of the determination coefficients R² (0.9869 and 0.9710 for the Li₄SiO₄ conversion and adsorption capacity models, respectively) and adjusted R² > 0.85 also denoted the goodness of the models selected.

As shown in Table 3, the effects that resulted high significance for the Li₄SiO₄ conversion (high values of sum of squares and p -value < 0.01) were the main effects of all factors, their quadratic terms, and the two-factor interactions AC (synthesis temperature-adsorption temperature) and CD (adsorption temperature-CO₂ concentration). In particular, the main effect of factor A-synthesis temperature had a sum of square two times greater than other main effects, indicating that the synthesis temperature can markedly affect the sorbent morphology (as can be seen by SEM analysis reported in Figure 2) and thus the conversion. Moreover, the interaction CD was found to be the most significant effect, showing the highest sum of squares among all the effects. This was related to the thermodynamic of the adsorption reaction on Li₄SiO₄, for which at 700 °C, the adsorption performance was high for 50 vol% of CO₂, whereas it was very low at 4 vol% due to the activation of the desorption process (Figure 4). Likewise, for the adsorption capacity (Table 4), the main effect of the A-synthesis temperature and the interactions AC (synthesis temperature-adsorption temperature) and CD (adsorption temperature-CO₂ concentration) resulted in the most significant effects since they had the highest sum of squares. Whereas the main effect of factor D-CO₂ concentration was almost not significant (p -value ≈ 0.05), and the factor B-K₂CO₃ content results were not significant. However, factor B was considered in the model to support hierarchy, since the interaction effect BD (K₂CO₃ content-CO₂ concentration) results were significant. BD significance indicates that the addition of K₂CO₃ to Li₄SiO₄ affected the adsorption capacity mostly in relation to the CO₂ content in the gas flow, and this was also noted in our previous study [27]. The addition of K₂CO₃ to Li₄SiO₄ more markedly improved the CO₂ uptake at low CO₂ concentrations (4 vol%) than at higher concentrations (50 vol%), since a high p_{CO_2} seemed to compensate for the lower diffusivity of the CO₂ in the product layer.

The adequacy of the obtained models was verified by diagnostic plots. For each response, the accordance between experimental data and predicted values was confirmed by the close distribution of run data to the line of the correspondent plot (Figure 7). The rela-

relationship between the factors, single or in interaction, can be visualized through the response model equations, which are reported in terms of actual factors in Equations (8) and (9).

$$Y_1 = 2249 - 6.245A + 2.147B - 3.336C + 10.78D + 1.070 \cdot 10^{-2}AC - 3.793 \cdot 10^{-2}AD - 7.818 \cdot 10^{-3}BD + 8.725 \cdot 10^{-3}CD + 3.906 \cdot 10^{-3}A^2 - 3.219 \cdot 10^{-2}B^2 - 7.940 \cdot 10^{-4}C^2 - 2.095 \cdot 10^{-2}D^2 - 6.757 \cdot 10^{-6}A^2C + 2.508 \cdot 10^{-5}A^2D \quad (8)$$

$$Y_2 = 6269 - 17.83A + 0.8924B - 9.099C + 34.64D + 3.151 \cdot 10^{-2}AC - 0.1169AD - 4.630 \cdot 10^{-2}BD + 2.625 \cdot 10^{-2}CD + 1.113 \cdot 10^{-2}A^2 - 2.959 \cdot 10^{-3}C^2 - 7.486 \cdot 10^{-2}D^2 - 1.990 \cdot 10^{-5}A^2C + 7.736 \cdot 10^{-5}A^2D \quad (9)$$

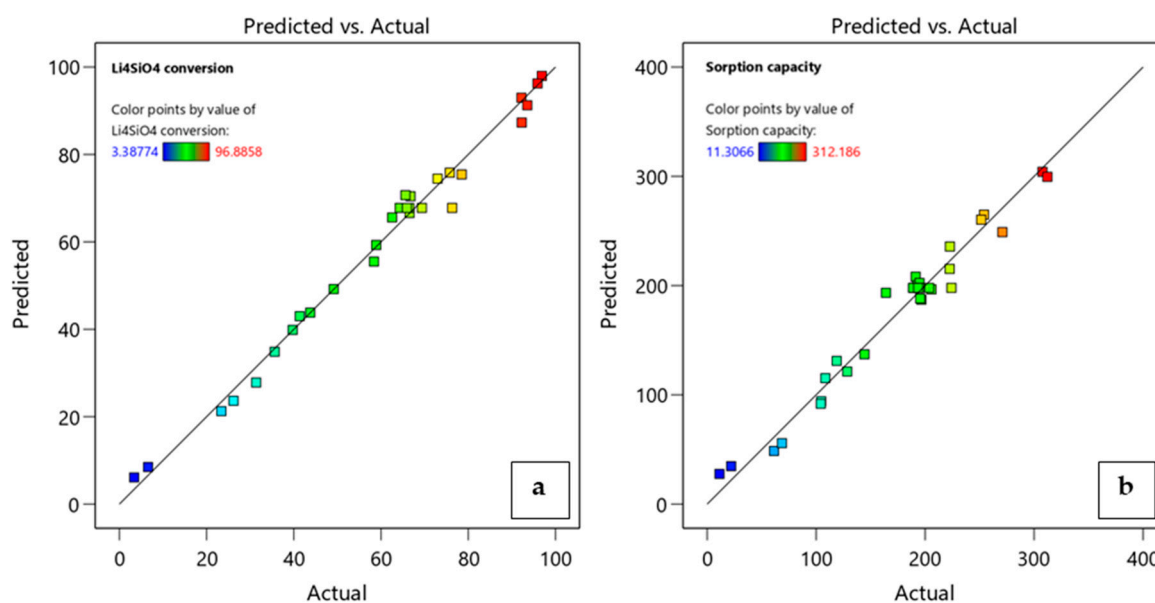


Figure 7. Diagnostic plots of predicted model values versus experimental data for (a) Li_4SiO_4 conversion and (b) adsorption capacity.

Three-dimensional response surface plots of the models for both responses are reported in Figures 8 and 9, and the relationships between factors and responses are discussed in the sections below. The 3D model graphs displayed the trend of both responses in the design space as a function of two significant variables, setting the other two variables at the center or factorial values.

3.3.1. Effect of Synthesis Temperature

According to the ANOVA results presented in Tables 3 and 4, synthesis temperature was an important variable that affected both the Li_4SiO_4 conversion and the adsorption capacity, and it demonstrated a quadratic effect on the responses (due to A^2 term) visible by a curvature in the model graphs of Figures 8a,b and 9a,b. However, its effect on the responses could not be considered individually as this factor presented interactions with adsorption temperature (AC, A^2C) and CO_2 concentration (AD, A^2D). Figures 8a and 9a display higher values of $X_{\text{Li}_4\text{SiO}_4}$ and adsorption capacity when the synthesis temperature was 600 °C, reaching about 92% and 270 mg/g, respectively, when the K_2CO_3 content was 25 wt%, the CO_2 in the treated gas was 27 vol% and the adsorption temperature was 600 °C. Moreover, these values increased as the CO_2 concentration increased from 4 to 50 vol% (Figures 8b and 9b), rising from nearly 40 to 100% and from 100 to 280 mg/g for $X_{\text{Li}_4\text{SiO}_4}$ and adsorption capacity, respectively (maintaining 25 wt% of K_2CO_3 and 600 °C of sorption temperature). These results were related both to sorbent morphology and adsorption reaction kinetics. As shown by the SEM analysis reported in Figure 2, a lower synthesis temperature led to a less sintered sorbent with smaller particle size

and thus to higher adsorption capacities and conversions [40,50–52]. Kim et al. [40] and Yang et al. [50] confirmed this trend, evidencing that Li_4SiO_4 sorbents produced at a low synthesis temperature (i.e., 600 °C) presented higher specific surface area and higher adsorption capacity. Moreover, when the CO_2 concentration increased from 4 to 50 vol%, the CO_2 concentration gradient between the bulk and the particle surface increased, so that increasing the amount of CO_2 adsorbed [17,26,53].

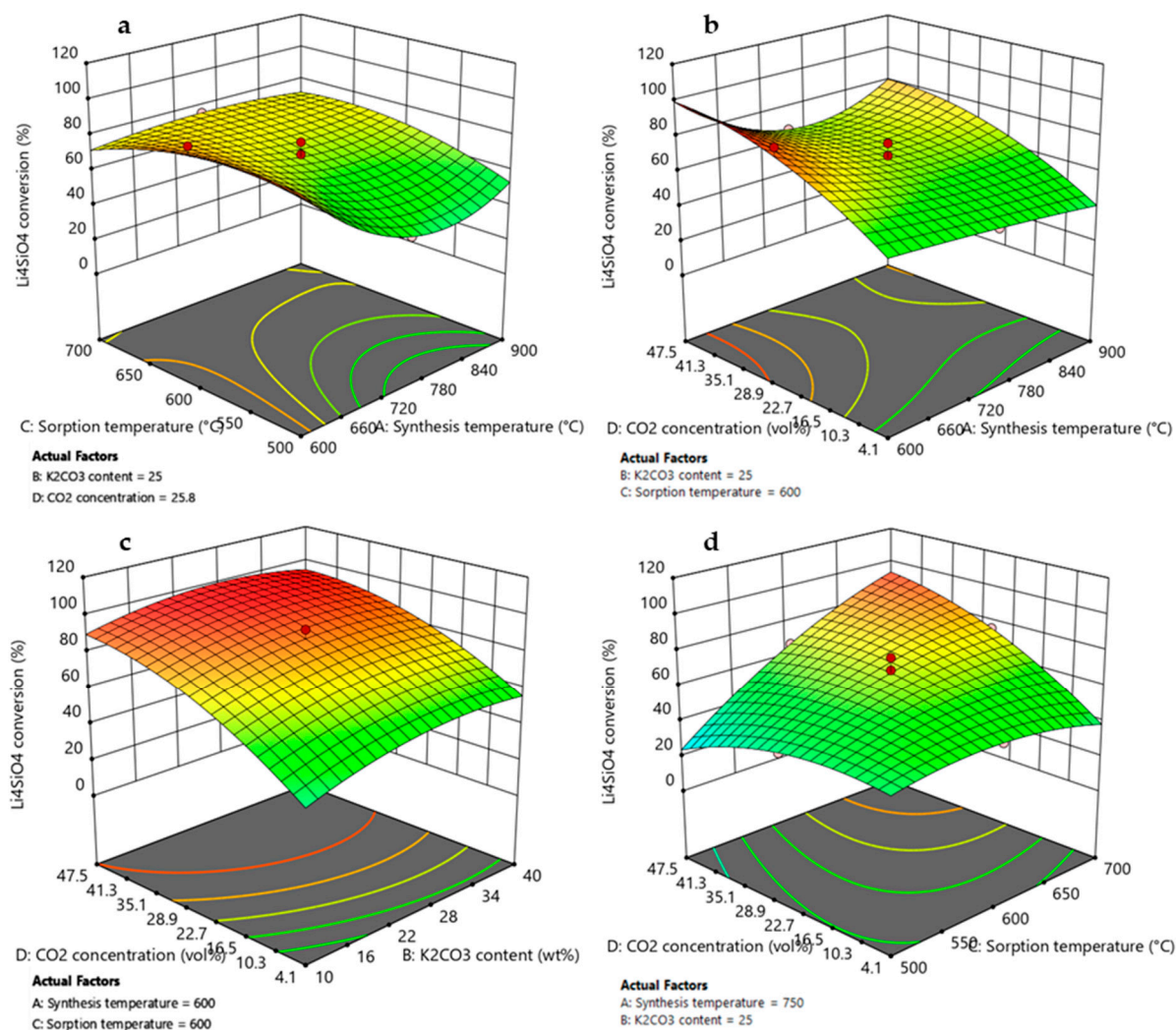


Figure 8. 3D response surface graphs obtained by RSM DoE for Li_4SiO_4 conversion as function of (a) synthesis temperature and sorption temperature, (b) synthesis temperature and CO_2 concentration, (c) K_2CO_3 content and CO_2 concentration, and (d) sorption temperature and CO_2 concentration. Red circles represent the Li_4SiO_4 conversion values obtained by experimental runs of the design matrix.

3.3.2. Effect of K_2CO_3 Content

As evident by ANOVA (Table 3), the variable K_2CO_3 content affected Li_4SiO_4 conversion, and it also demonstrated a quadratic effect on the response (due to the B^2 term), visible by a slight curvature in the model graph of Figure 8c. On the contrary, for the adsorption capacity, the factor K_2CO_3 content results were not significant (Table 4), and this is shown by a linear contour plot in Figure 9c. This different result can be explained by considering that an increase in K_2CO_3 content helped the reaction kinetics by reducing diffusion resistance through the product layer that covered the sorbent particles, leading to higher Li_4SiO_4 conversion. Nevertheless, higher values of K_2CO_3 content reduced the amount of active sorbent (Li_4SiO_4 , which actually reacted with CO_2), leading to a lower adsorption capacity [44]. However, the interaction effect BD (K_2CO_3 content- CO_2 concen-

tration) results were significant, and this is represented on 3D response surface plots by a slight curvature of the surface when CO₂ concentration varies from 4 to 50 vol%. The addition of K₂CO₃ to Li₄SiO₄ more markedly improved the adsorption performance at low CO₂ concentrations, where the diffusion resistance was high due to the lower gradient for the CO₂ mass transfer into the product layer. Li₄SiO₄ conversion and adsorption capacity increased from 40 to 55% and from 135 to 160 mg/g, respectively, when the K₂CO₃ content increased from 10 to 40 wt % for 4 vol% of CO₂ in the treated gas (considering synthesis and adsorption temperature of 600 °C). Whereas at higher p_{CO_2} , the increasing concentration gradient compensated for the lower diffusivity of the CO₂ in the product layer [27,30]. When the CO₂ concentration was 50 vol% and the K₂CO₃ content increased from 10 to 40 wt %, Li₄SiO₄ conversion ranged from 90-95%, while the adsorption capacity remained almost constant to 260 mg/g (synthesis and adsorption temperature set to 600 °C). The same effect has been observed by [30], which found that the optimum amount of K₂CO₃ for maximizing CO₂ uptake depended on the CO₂ concentration in the treated gas.

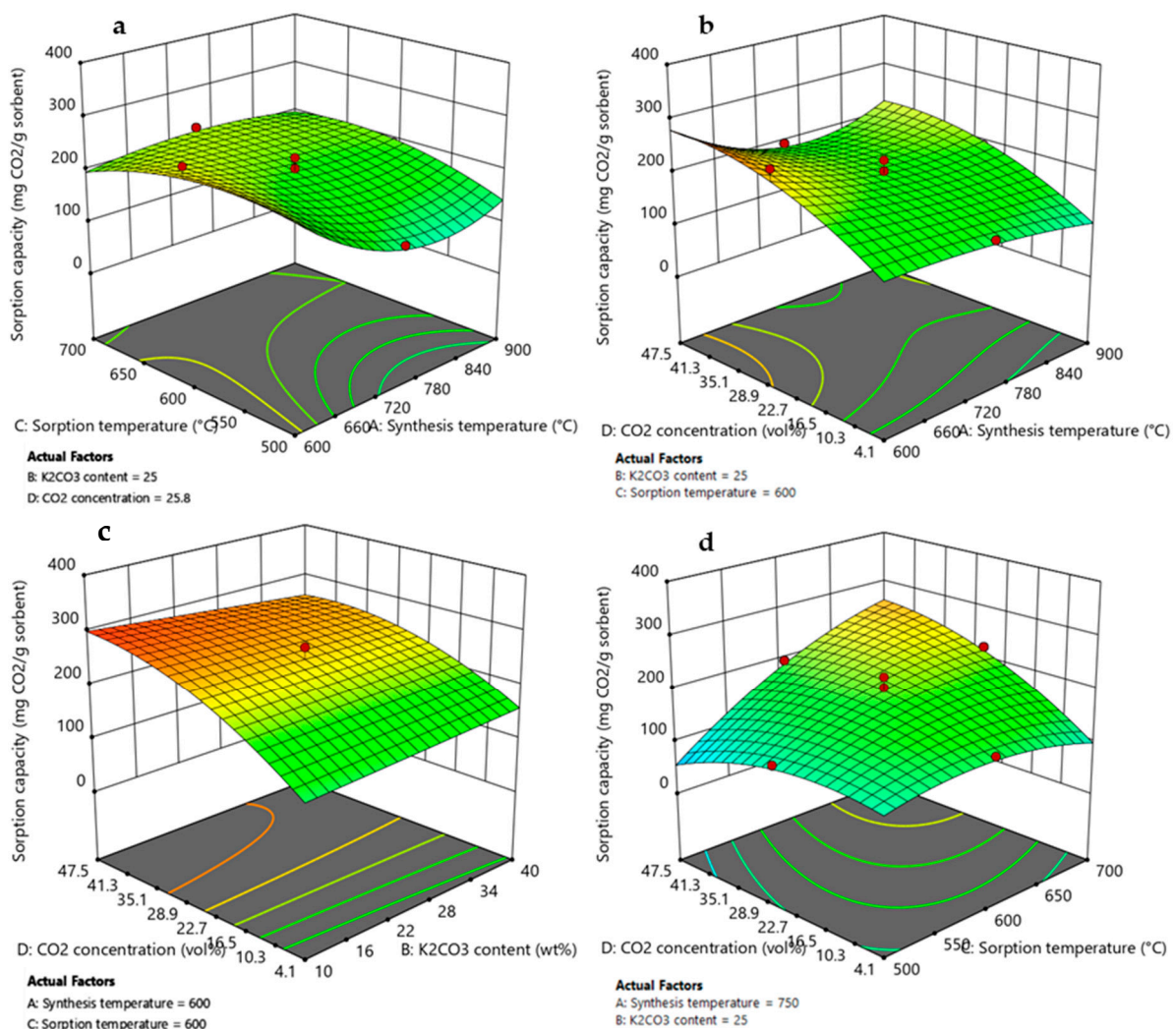


Figure 9. 3D response surface graphs obtained by RSM DoE for adsorption capacity as function of (a) synthesis temperature and sorption temperature, (b) synthesis temperature and CO₂ concentration, (c) K₂CO₃ content and CO₂ concentration, and (d) sorption temperature and CO₂ concentration. Red circles represent the Li₄SiO₄ conversion values obtained by experimental runs of the design matrix.

3.3.3. Effect of Adsorption Temperature and CO₂ Concentration

Based on the ANOVA results (Tables 3 and 4) and the model's equations (Equations (8) and (9)), the term mostly affecting either Li₄SiO₄ conversion or adsorption capacity was the two-

factor interaction CD (adsorption temperature-CO₂ concentration). It showed the highest sum of squares and a positive effect on the responses (the coefficient in the model's equations was the highest in terms of coded factors and has a positive sign). The positive effect could be noted in response surface graphs of Figures 7d and 8d, where both Li₄SiO₄ conversion and adsorption capacity increased with increasing the adsorption temperature and CO₂ concentration. This term is strictly correlated to the adsorption reaction thermodynamic since the first condition for obtaining high CO₂ removal performance is to work in a region where adsorption is favored [17,26,53]. It is important to highlight that, at 4 vol% CO₂, both the Li₄SiO₄ conversion and adsorption capacity showed a decrease by increasing the adsorption temperature from 500 to 700 °C (Figures 7d and 8d). This was associated with the adsorption reaction equilibrium, for which at 500 °C the adsorption process was favored, whereas at 700 °C, the desorption process was activated (Figure 4) [17,27,54].

3.4. Optimization and Validation Tests

The process of CO₂ capture using K₂CO₃-doped Li₄SiO₄ sorbents requires high CO₂ adsorption capacities to be efficient for practical applications. Moreover, high Li₄SiO₄ conversions are necessary for the process to be economically feasible. Therefore, the parametric models obtained by RSM analysis were used for a multi-objective optimization that allows to predict the optimal combination of variables for maximizing both the Li₄SiO₄ conversion and the adsorption capacity. As evidenced by response surface plots, by varying input parameters the two responses did not behave the same way. As previously observed, K₂CO₃ kinetically improved the sorbent performance in terms of conversion but, on the other hand, it represents an inert that reduces the amount of active sorbent (Li₄SiO₄), with a consequent reduction of adsorption capacity for high K₂CO₃ content [44]. The optimization was carried out for three different CO₂ concentrations (4, 27, 50 vol%), letting the other factors (synthesis temperature, K₂CO₃ content, and adsorption temperature) vary in their range and maximizing the two responses. The optimum conditions for the process variables and the predicted values for the responses, obtained for the three different CO₂ concentrations by numerical optimization, are reported in Tables 5 and 6.

Table 5. Optimization results of the process variables.

Process Variable	Optimum Value		
	4 vol% CO ₂	27 vol% CO ₂	50 vol% CO ₂
A-Synthesis temperature (°C)	600	600	600
B-K ₂ CO ₃ content (wt%)	36.9	28.5	17.1
C-Adsorption temperature (°C)	500	557	662

Table 6. Predicted and experimental response values at optimum conditions.

CO ₂ Concentration	Response	Predicted Value	Experimental Result	Error (%)
4 vol%	Y ₁ : Li ₄ SiO ₄ conversion (%)	75.6	73.2	1.86
	Y ₂ : Adsorption capacity (mg/g)	206.0	196.4	3.44
27 vol%	Y ₁ : Li ₄ SiO ₄ conversion (%)	89.9	83.7	5.15
	Y ₂ : Adsorption capacity (mg/g)	252.2	239.2	3.41
50 vol%	Y ₁ : Li ₄ SiO ₄ conversion (%)	98.5	94.3	4.25
	Y ₂ : Adsorption capacity (mg/g)	300.1	295.6	1.47

For each different optimization (at different CO₂ concentrations), the models predicted an optimum working point that was different from all the runs (factorial, center, and axial points) already performed during experimentation, and with predicted values of Li₄SiO₄ conversion and adsorption capacity higher than the values already observed in the experimental runs. This suggests a good models predictivity. All the optimum values obtained for the process variables (Table 5) show that a synthesis temperature of

600 °C would lead to the highest CO₂ removal sorbent performance, whatever the CO₂ concentration. This was probably due to the less sintered structure with smaller particle size of the sorbent (Figure 2), as explained in Section 3.3.1. The amount of K₂CO₃ required to maximize both Y₁ and Y₂ decreased as the CO₂ concentration increased. This result could be explained as a consequence of Fick's law for diffusive mass transfer; the higher the CO₂ concentration is, the higher the driving force (concentration gradient between the bulk and the particle surface) is for diffusion. Thus, the amount of K₂CO₃ required to improve CO₂ diffusivity through the product layer was lower. Then, for the low CO₂ concentration, it is necessary to work with high K₂CO₃ content to contrast the low driving force with an improved diffusivity coefficient [27,30]. Similar results have been found by [30], which observed that the optimum K₂CO₃ content for maximizing CO₂ uptake varied with CO₂ concentration. However, no systematic study has been performed that takes into account the effect of adsorption temperature, which significantly affects sorption performance and, consequently, the optimal K₂CO₃ amount. On the contrary, the optimum adsorption temperature required to maximize both responses increases with increasing CO₂ concentration. This result is associated with the adsorption reaction equilibrium, so the optimum temperature would tend to be as close as possible to the thermodynamic equilibrium temperature, which increases as CO₂ concentration increases (Figure 4), as widely discussed in Section 3.3.3.

To evaluate the model adequacy and the validity of the optimization procedure, multiple confirmation runs were performed. Three additional experiments for each optimization at different CO₂ concentrations were carried out under the proposed optimal conditions reported in Table 5. The average values of the three repeated experiments are presented in Table 6, together with the calculated average error between the predicted values and the experimental validation tests. As shown, the experimental and predicted responses values are in agreement, with an error range of about 1–5%. Therefore, the obtained RSM models can correlate the process variables to the Li₄SiO₄ conversion and the adsorption capacity with high accuracy. These results demonstrate the suitability of the RSM DoE methodology for the modeling and optimization of the CO₂ capture process on K₂CO₃-doped lithium orthosilicate sorbents.

The optimized sorbents, for the three CO₂ concentrations investigated, displayed excellent adsorption capacity and conversion in each sorption condition. Notably, at 4 vol% of CO₂, the optimized sorbent could capture 196.4 mg CO₂/g sorbent (corresponding to a conversion of almost 73%) after 120 min of adsorption; the adsorption capacity increased to 239.2 and 295.6 mg/g (about 84 and 94% of Li₄SiO₄ conversion) with increasing the CO₂ concentration to 27 and 50 vol%, respectively. These CO₂ uptakes are comparable with the adsorption capacities of alkali doped-Li₄SiO₄ sorbents reported in the recent literature [28,29,31–34], demonstrating their effectiveness, especially considering the low CO₂ concentration (4 vol%) in the flue gas used in this work for the experimentations, while all the other sorbents were tested at 15 or 100 vol% of CO₂. For example, the adsorption capacity attained by [29,30,34] for K₂CO₃-doped Li₄SiO₄ sorbents varied between values of about 240 and 280 mg CO₂/g sorbent in a 15–20 vol% CO₂ atmosphere, similar to our optimized sorbent (239.2 mg/g in 27 vol% CO₂).

The doped-Li₄SiO₄ sorbent optimized for maximum conversion and adsorption capacity, considering a CO₂ concentration in the treated gas of 4 vol%, was subjected to cyclic CO₂ adsorption/desorption tests to evaluate its regenerability and stability. These properties are essential for a good CO₂ sorbent in view of its use in industrial processes, such as in a fixed bed for capturing CO₂ emissions from exhaust flue gas from gas turbines. Multiple adsorption (CO₂/N₂ mixture of 4/96 vol%) and desorption (100 vol% N₂) cycles were performed in the TGA system at 1 bar. The adsorption temperature was set to 500 °C (as obtained by the optimization results) and maintained for 60 min; then, the desorption process was carried out elevating the temperature to 700 °C for 30 min. The results are shown in Figure 10, evidencing an excellent regeneration capacity for 20 adsorption/desorption cycles without activity decay.

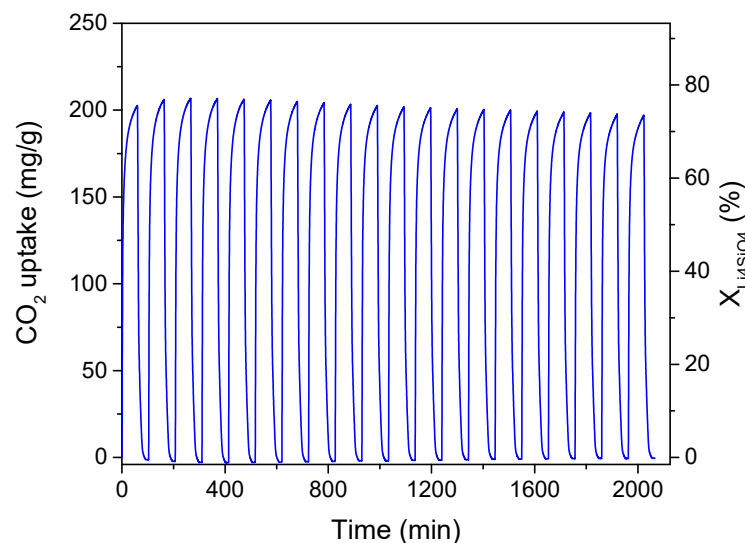


Figure 10. Cyclic adsorption/desorption performance of optimized K_2CO_3 -doped Li_4SiO_4 (synthesis temperature $600\text{ }^\circ\text{C}$, 36.9 wt% K_2CO_3). Test conditions: adsorption at $500\text{ }^\circ\text{C}$ for 60 min in 4 vol% CO_2 stream; desorption at $700\text{ }^\circ\text{C}$ for 30 min in 100 vol% N_2 .

The CO_2 uptake of the first cycle was about 203 mg/g and remained almost constant for the subsequent cycles. This performance resulted in values higher or almost equal to those obtained for similar K_2CO_3 -doped sorbents. Zhang et al. [30] reached only $163.1\text{ mg CO}_2/\text{g}$, and this value reduced to 97.6 mg/g after 22 adsorption/desorption cycles in 20 vol% CO_2 . Wang et al. [29] presented a sorbent that was able to adsorb $188.0\text{ mg CO}_2/\text{g}$ in the first cycle, while its adsorption capacity decreased to 159.4 mg/g after 22 cycles. The sol-gel prepared Li_4SiO_4 of Cui et al. [33] displayed good stability for over 20 cycles when doped with K_2CO_3 maintaining a CO_2 uptake of 310 mg/g in 15 vol% CO_2 .

The high adsorption capacities and the good regeneration and stability obtained at very low CO_2 content suggest that K_2CO_3 -doped Li_4SiO_4 sorbents could be suitable for CO_2 capture in industrial applications, such as in gas-fired power plants. Furthermore, the RSM methodology could be effectively used for tailoring the sorbent synthesis conditions, thus optimizing its adsorption performance for different adsorption conditions. Improvements to the parametric modeling and study of CO_2 adsorption by Li_4SiO_4 -based sorbents could concern the application of RSM DoE methodology, scaling up the production process and the testing conditions to obtain representative predictions of the sorbent behavior. Moreover, the long-term stability and sorbent's regeneration efficiency could be investigated as DoE responses obtaining predictive models of such important characteristics of the sorbent.

4. Conclusions

In this work, a new approach for the production of K_2CO_3 -doped Li_4SiO_4 sorbents for CO_2 capture at high temperatures was investigated and validated for different operating conditions. The Design of Experiments methodology was applied to study and identify the synthesis and operating variables that mostly affect the adsorption performance of the produced sorbents, defined in terms of Li_4SiO_4 conversion and adsorption capacity. Four operating variables were systematically varied: synthesis temperature, K_2CO_3 content, adsorption temperature, and CO_2 concentration in the treated gas. Using the Response Surface Method, non-linear parametric models were found capable of accurately fitting the experimental data, allowing to predict the optimal combination of variables for maximizing both Li_4SiO_4 conversion and adsorption capacity. The optimization results indicated that sorbents synthesized at $600\text{ }^\circ\text{C}$ ensured the maximum CO_2 uptake for different CO_2 concentrations (4, 27, and 50 vol%), due to a less sintered microstructure. The optimized sorbents showed an adsorption capacity of 196.4 mg/g at $500\text{ }^\circ\text{C}$ and 4 vol%, which increased to 295.6 mg/g when the CO_2 concentration was 50 vol% and the adsorption temperature was

662 °C. The present study suggests that the developed parametric RSM models are effectively capable of predicting the sorbent performance and indicating the proper synthesis condition for maximizing the CO₂ capture at each operating condition, thus providing information for a process scale-up. Moreover, the produced K₂CO₃-doped Li₄SiO₄ sorbents demonstrated high adsorption capacity even at very low CO₂ concentrations, making them suitable for CO₂ removal in industrial processes. Future developments of this research activity could involve a parametric study of the effect of different doping agents on the sorbent's adsorption capacity, as well as an investigation into the impact of steam in the gas stream to be treated.

Author Contributions: Conceptualization, M.P.; methodology, E.S., S.V., and M.P.; software, E.S. and F.F.; validation, E.S.; formal analysis, F.F.; investigation, E.S.; resources, M.P.; data curation, E.S. and F.F.; writing—original draft preparation, E.S. and F.F.; writing—review and editing, E.S. and M.P.; visualization, E.S. and S.V.; supervision, S.V. and M.P.; project administration, M.P.; funding acquisition, M.P. All authors have read and agreed to the published version of the manuscript.

Funding: This research received no external funding.

Institutional Review Board Statement: Not applicable.

Informed Consent Statement: Not applicable.

Data Availability Statement: The raw data supporting the conclusions of this article will be made available by the authors on request.

Acknowledgments: This research is supported by the Ministry of University and Research (MUR) as part of the PON 2014–2020 “Research and Innovation” resources-Green/Innovation Action-DM MUR 1062/2021.

Conflicts of Interest: The authors declare no conflicts of interest.

References

1. Gunawardene, O.H.P.; Gunathilake, C.A.; Vikrant, K.; Amaraweera, S.M. Carbon Dioxide Capture through Physical and Chemical Adsorption Using Porous Carbon Materials: A Review. *Atmosphere* **2022**, *13*, 397. [[CrossRef](#)]
2. Rahimi, K.; Riahi, S.; Abbasi, M.; Fakhroueian, Z. Modification of Multi-Walled Carbon Nanotubes by 1,3-Diaminopropane to Increase CO₂ Adsorption Capacity. *J. Environ. Manag.* **2019**, *242*, 81–89. [[CrossRef](#)]
3. Mikolajewicz, U.; Grö, M.; Ernst, A.E.; Ae, M.-R.; Schurgers, G.; Miren, A.E.; Ae, V.; Winguth, A.M.E. Long-Term Effects of Anthropogenic CO₂ Emissions Simulated with a Complex Earth System Model. *Clim. Dyn.* **2007**, *28*, 599–633. [[CrossRef](#)]
4. Bhattacharjee, P.K. Global Warming Impact on the Earth. *Int. J. Environ. Sci. Dev.* **2010**, *1*, 219–220. [[CrossRef](#)]
5. Yoro, K.O.; Daramola, M.O. CO₂ Emission Sources, Greenhouse Gases, and the Global Warming Effect. *Adv. Carbon Capture Methods Technol. Appl.* **2020**, 3–28. [[CrossRef](#)]
6. Holechek, J.L.; Geli, H.M.E.; Sawalhah, M.N.; Valdez, R. A Global Assessment: Can Renewable Energy Replace Fossil Fuels by 2050? *Sustainability* **2022**, *14*, 4792. [[CrossRef](#)]
7. Gernaat, D.E.H.J.; de Boer, H.S.; Daioglou, V.; Yalaw, S.G.; Müller, C.; van Vuuren, D.P. Climate Change Impacts on Renewable Energy Supply. *Nat. Clim. Chang.* **2021**, *11*, 119–125. [[CrossRef](#)]
8. Okiemute Akpasi, S.; Makarfi Isa, Y. Review of Carbon Capture and Methane Production from Carbon Dioxide. *Atmosphere* **2022**, *13*, 1958. [[CrossRef](#)]
9. Fawzy, S.; Osman, A.I.; Doran, J.; Rooney, D.W. Strategies for Mitigation of Climate Change: A Review. *Environ. Chem. Lett.* **2020**, *18*, 2069–2094. [[CrossRef](#)]
10. Rajendran, A.; Subraveti, S.G.; Pai, K.N.; Prasad, V.; Li, Z. How Can (or Why Should) Process Engineering Aid the Screening and Discovery of Solid Sorbents for CO₂ Capture? *Acc. Chem. Res.* **2023**, *56*, 2354–2365. [[CrossRef](#)]
11. Dai, M.; Xie, J.; Li, X.; Gao, X. Investment Evaluation of CCUS Retrofitting for Coal-to-Liquid Industry in China. *Atmosphere* **2023**, *14*, 1737. [[CrossRef](#)]
12. Wilfong, W.C.; Ji, T.; Bao, Z.; Zhai, H.; Wang, Q.; Duan, Y.; Soong, Y.; Li, B.; Shi, F.; Gray, M.L. Big Data Analysis and Technical Review of Regeneration for Carbon Capture Processes. *Energy Fuels* **2023**, *37*, 11497–11531. [[CrossRef](#)]
13. Zhang, Z.; Yang, S.; Zhang, D.; Shen, B.; Li, Z.; Ma, J.; Liu, L. Fabrication of Robust CaO-Based Sorbent via Entire Utilization of MSW Incineration Bottom Ash for CO₂ Capture. *Sep. Purif. Technol.* **2023**, *307*, 122795. [[CrossRef](#)]
14. Ma, X.; Li, Y.; Duan, L.; Anthony, E.; Liu, H. CO₂ Capture Performance of Calcium-Based Synthetic Sorbent with Hollow Core-Shell Structure under Calcium Looping Conditions. *Appl. Energy* **2018**, *225*, 402–412. [[CrossRef](#)]
15. Li, C.; Gong, X.; Zhang, H.; Zhang, Y.; Yang, M.; Chen, B. CO₂ Capture Performance of CaO-Based Sorbent Modified with Torrefaction Condensate during Calcium Looping Cycles. *Chem. Eng. J.* **2023**, *469*, 144004. [[CrossRef](#)]

16. Peltzer, D.; Salazar Hoyos, L.A.; Faroldi, B.; Múnera, J.; Cornaglia, L. Comparative Study of Lithium-Based CO₂ Sorbents at High Temperature: Experimental and Modeling Kinetic Analysis of the Carbonation Reaction. *J. Environ. Chem. Eng.* **2020**, *8*, 104173. [[CrossRef](#)]
17. Tong, Y.; Chen, S.; Huang, X.; He, Y.; Chen, J.; Qin, C. CO₂ Capture by Li₄SiO₄ Sorbents: From Fundamentals to Applications. *Sep. Purif. Technol.* **2022**, *301*, 121977. [[CrossRef](#)]
18. Seggiani, M.; Stefanelli, E.; Puccini, M.; Vitolo, S. CO₂ Sorption/Desorption Performance Study on K₂CO₃-Doped Li₄SiO₄-Based Pellets. *Chem. Eng. J.* **2018**, *339*, 51–60. [[CrossRef](#)]
19. Stefanelli, E.; Vitolo, S.; Puccini, M. Single-Step Fabrication of Templated Li₄SiO₄-Based Pellets for CO₂ Capture at High Temperature. *J. Environ. Chem. Eng.* **2022**, *10*, 108389. [[CrossRef](#)]
20. Peltzer, D.; Múnera, J.; Cornaglia, L.; Strumendo, M. Characterization of Potassium Doped Li₂ZrO₃ Based CO₂ Sorbents: Stability Properties and CO₂ Desorption Kinetics. *Chem. Eng. J.* **2017**, *336*, 1–11. [[CrossRef](#)]
21. Lara-Garcia, H.; Alcántar-Vázquez, B.; Duan, Y.; Pfeiffer, H. CO Chemical Capture on Lithium Cuprate, through a Consecutive CO Oxidation and Chemisorption Bifunctional Process. *J. Phys. Chem. C* **2016**, *120*, 3798–3806. [[CrossRef](#)]
22. Al-Mamoori, A.; Hameed, M.; Saoud, A.; Al-Ghamdi, T.; Al-Naddaf, Q.; AlWakwak, A.A.; Baamran, K. Development of Sodium-Based Borate Adsorbents for CO₂ Capture at High Temperatures. *Ind. Eng. Chem. Res.* **2023**, *62*, 3695–3704. [[CrossRef](#)]
23. Ji, G.; Yang, H.; Memon, M.Z.; Gao, Y.; Qu, B.; Fu, W.; Olguin, G.; Zhao, M.; Li, A. Recent Advances on Kinetics of Carbon Dioxide Capture Using Solid Sorbents at Elevated Temperatures. *Appl. Energy* **2020**, *267*, 114874. [[CrossRef](#)]
24. Hu, Y.; Liu, W.; Yang, Y.; Qu, M.; Li, H. CO₂ Capture by Li₄SiO₄ Sorbents and Their Applications: Current Developments and New Trends. *Chem. Eng. J.* **2019**, *359*, 604–625. [[CrossRef](#)]
25. Yan, X.; Li, Y.; Ma, X.; Zhao, J.; Wang, Z.; Yan, X.; Li, Y.; Ma, X.; Zhao, J.; Wang, Z. Performance of Li₄SiO₄ Material for CO₂ Capture: A Review. *Int. J. Mol. Sci.* **2019**, *20*, 928. [[CrossRef](#)]
26. Yang, Y.; Dai, P.; Chen, Z.; Sun, X.; Ren, X. Kinetic and Thermodynamic Investigations on the Cyclic CO₂ Adsorption-Desorption Processes of Lithium Orthosilicate. *Chem. Eng. J.* **2023**, *468*, 143679. [[CrossRef](#)]
27. Stefanelli, E.; Puccini, M.; Vitolo, S.; Seggiani, M. CO₂ Sorption Kinetic Study and Modeling on Doped-Li₄SiO₄ under Different Temperatures and CO₂ Partial Pressures. *Chem. Eng. J.* **2020**, *379*, 122307. [[CrossRef](#)]
28. Zhou, Z.; Wang, K.; Yin, Z.; Zhao, P.; Su, Z.; Sun, J. Molten K₂CO₃-Promoted High-Performance Li₄SiO₄ Sorbents at Low CO₂ Concentrations. *Thermochim. Acta* **2017**, *655*, 284–291. [[CrossRef](#)]
29. Wang, J.; Chen, K.; Wang, Y.; Lei, J.; Alsubaie, A.; Ning, P.; Wen, S.; Zhang, T.; Almalki, A.S.A.; Alhadhrami, A.; et al. Effect of K₂CO₃ Doping on CO₂ Sorption Performance of Silicate Lithium-Based Sorbent Prepared from Citric Acid Treated Sediment. *Chinese J. Chem. Eng.* **2022**, *51*, 10–20. [[CrossRef](#)]
30. Zhang, T.; Li, M.; Ning, P.; Jia, Q.; Wang, Q.; Wang, J. K₂CO₃ Promoted Novel Li₄SiO₄-Based Sorbents from Sepiolite with High CO₂ Capture Capacity under Different CO₂ Partial Pressures. *Chem. Eng. J.* **2020**, *380*, 122515. [[CrossRef](#)]
31. Jia, Y.; Wei, J.; Yuan, Y.; Zhou, X.; Geng, L.; Liao, L. High Temperature Capture of Low Concentration CO₂ by Na/Ca-Doped Lithium Orthosilicate with KIT-6 as Precursor. *Mater. Today Commun.* **2022**, *33*, 104685. [[CrossRef](#)]
32. Mu, Y.; Zhang, M.; Guo, M. Na-Doped Li₄SiO₄ as an Efficient Sorbent for Low-Concentration CO₂ Capture at High Temperature: Superior Adsorption and Rapid Kinetics Mechanism. *Sep. Purif. Technol.* **2025**, *352*, 128268. [[CrossRef](#)]
33. Cui, H.; Li, X.; Chen, H.; Gu, X.; Cheng, Z.; Zhou, Z. Sol-Gel Derived, Na/K-Doped Li₄SiO₄-Based CO₂ Sorbents with Fast Kinetics at High Temperature. *Chem. Eng. J.* **2020**, *382*, 122807. [[CrossRef](#)]
34. Ma, L.; Chen, S.; Qin, C.; Chen, S.; Yuan, W.; Zhou, X.; Ran, J. Understanding the Effect of H₂S on the Capture of CO₂ Using K-Doped Li₄SiO₄ Sorbent. *Fuel* **2021**, *283*, 119364. [[CrossRef](#)]
35. Bararpour, S.T.; Karami, D.; Mahinpey, N. Investigation of the Effect of Alumina-Aerogel Support on the CO₂ Capture Performance of K₂CO₃. *Fuel* **2019**, *242*, 124–132. [[CrossRef](#)]
36. Thouchprasitchai, N.; Pintuyothin, N.; Pongstabodee, S. Optimization of CO₂ Adsorption Capacity and Cyclical Adsorption/Desorption on Tetraethylenepentamine-Supported Surface-Modified Hydrotalcite. *J. Environ. Sci.* **2018**, *65*, 293–305. [[CrossRef](#)]
37. Amiri, M.; Shahhosseini, S.; Ghaemi, A. Optimization of CO₂ Capture Process from Simulated Flue Gas by Dry Regenerable Alkali Metal Carbonate Based Adsorbent Using Response Surface Methodology. *Energy Fuels* **2017**, *31*, 5286–5296. [[CrossRef](#)]
38. Amiri, M.; Shahhosseini, S. Optimization of CO₂ Capture from Simulated Flue Gas Using K₂CO₃/Al₂O₃ in a Micro Fluidized Bed Reactor. *Energy Fuels* **2018**, *32*, 7978–7990. [[CrossRef](#)]
39. Oehlert, G.W. *A First Course in Design and Analysis of Experiments*, 1st ed.; W. H. Freeman: New York, NY, USA, 2000; ISBN 0-7167-3510-5.
40. Kim, H.; Jang, H.D.; Choi, M. Facile Synthesis of Macroporous Li₄SiO₄ with Remarkably Enhanced CO₂ Adsorption Kinetics. *Chem. Eng. J.* **2015**, *280*, 132–137. [[CrossRef](#)]
41. Chang, C.C.; Wang, C.C.; Kumta, P.N. Chemical Synthesis and Characterization of Lithium Orthosilicate (Li₄SiO₄). *Mater. Des.* **2001**, *22*, 617–623. [[CrossRef](#)]
42. Cruz, D.; Bulbulian, S.; Lima, E.; Pfeiffer, H. Kinetic Analysis of the Thermal Stability of Lithium Silicates (Li₄SiO₄ and Li₂SiO₃). *J. Solid State Chem.* **2006**, *179*, 909–916. [[CrossRef](#)]
43. Pfeiffer, H.; Bosch, P.; Bulbulian, S. Synthesis of Lithium Silicates. *J. Nucl. Mater.* **1998**, *257*, 309–317. [[CrossRef](#)]

44. Seggiani, M.; Puccini, M.; Vitolo, S. Alkali Promoted Lithium Orthosilicate for CO₂ Capture at High Temperature and Low Concentration. *Int. J. Greenh. Gas Control* **2013**, *17*, 25–31. [[CrossRef](#)]
45. Pavri, R.; Moore, G.D. *Gas Turbine Emissions and Control*; GER-4211; GE Energy Services: Atlanta, Georgia, 2001.
46. Cheng, C.-Y.; Kuo, C.-C.; Yang, M.-W.; Zhuang, Z.-Y.; Lin, P.-W.; Chen, Y.-F.; Yang, H.-S.; Chou, C.-T. CO₂ Capture from Flue Gas of a Coal-Fired Power Plant Using Three-Bed PSA Process. *Energies* **2021**, *14*, 3582. [[CrossRef](#)]
47. Amann, J.M.G.; Bouallou, C. CO₂ Capture from Power Stations Running with Natural Gas (NGCC) and Pulverized Coal (PC): Assessment of a New Chemical Solvent Based on Aqueous Solutions of N-Methyldiethanolamine + Triethylene Tetramine. *Energy Procedia* **2009**, *1*, 909–916. [[CrossRef](#)]
48. David, E.; Stanciu, V.; Sandra, C.; Armeanu, A.; Niculescu, V. Exhaust Gas Treatment Technologies for Pollutant Emission Abatement from Fossil Fuel Power Plants. *WIT Trans. Ecol. Environ.* **2007**, *102*, 923–932. [[CrossRef](#)]
49. Seggiani, M.; Puccini, M.; Vitolo, S. High-Temperature and Low Concentration CO₂ Sorption on Li₄SiO₄ Based Sorbents: Study of the Used Silica and Doping Method Effects. *Int. J. Greenh. Gas Control* **2011**, *5*, 741–748. [[CrossRef](#)]
50. Yang, Y.; Yao, S.; Liu, W.; Hu, Y.; Li, Q.; Li, Z.; Zhou, S.; Zhou, Z. Novel Synthesis of Tailored Li₄SiO₄-Based Microspheres for Ultrafast CO₂ Adsorption. *Fuel Process. Technol.* **2021**, *213*, 106675. [[CrossRef](#)]
51. Izquierdo, M.T.; Turan, A.; García, S.; Maroto-Valer, M.M. Optimization of Li₄SiO₄ Synthesis Conditions by a Solid State Method for Maximum CO₂ Capture at High Temperature. *J. Mater. Chem. A* **2018**, *6*, 3249–3257. [[CrossRef](#)]
52. Izquierdo, M.T.; Gasquet, V.; Sansom, E.; Ojeda, M.; Garcia, S.; Maroto-Valer, M.M. Lithium-Based Sorbents for High Temperature CO₂ Capture: Effect of Precursor Materials and Synthesis Method. *Fuel* **2018**, *230*, 45–51. [[CrossRef](#)]
53. Chen, S.; Dai, J.; Qin, C.; Yuan, W.; Manovic, V. Adsorption and Desorption Equilibrium of Li₄SiO₄-Based Sorbents for High-Temperature CO₂ Capture. *Chem. Eng. J.* **2022**, *429*, 132236. [[CrossRef](#)]
54. Kaniwa, S.; Yoshino, M.; Niwa, E.; Yashima, M.; Hashimoto, T. Analysis of Chemical Reaction between Li₄SiO₄ and CO₂ by Thermogravimetry under Various CO₂ Partial Pressures—Clarification of CO₂ Partial Pressure and Temperature Region of CO₂ Absorption. *Mater. Res. Bull.* **2017**, *94*, 134–139. [[CrossRef](#)]

Disclaimer/Publisher’s Note: The statements, opinions and data contained in all publications are solely those of the individual author(s) and contributor(s) and not of MDPI and/or the editor(s). MDPI and/or the editor(s) disclaim responsibility for any injury to people or property resulting from any ideas, methods, instructions or products referred to in the content.